

**EUR 4136 e**

EUROPEAN ATOMIC ENERGY COMMUNITY — EURATOM

**STUDIES ON THE TERNARY SYSTEM  $\text{UO}_2 - \text{U}_3\text{O}_8 - \text{PuO}_2$**

by

U. BENEDICT and C. SARI

1970



Joint Nuclear Research Center  
Karlsruhe Establishment — Germany

European Transuranium Institute

## LEGAL NOTICE

This document was prepared under the sponsorship of the Commission of the European Communities.

Neither the Commission of the European Communities, its contractors nor any person acting on their behalf:

make any warranty or representation, express or implied, with respect to the accuracy, completeness or usefulness of the information contained in this document, or that the use of any information, apparatus, method or process disclosed in this document may not infringe privately owned rights; or

assume any liability with respect to the use of, or for damages resulting from the use of any information, apparatus, method or process disclosed in this document.

This report is on sale at the addresses listed on cover page 4

at the price of FF 6.65	FB 60.—	DM 4.40	Lit. 750	Fl. 4.30
-------------------------	---------	---------	----------	----------

When ordering, please quote the EUR number and the title which are indicated on the cover of each report.

Printed by Van Muysewinkel  
Brussels, February 1970.

This document was reproduced on the basis of the best available copy.

## EUR 4136 e

STUDIES ON THE TERNARY SYSTEM  $UO_2-U_3O_8-PuO_2$   
by U. BENEDICT and C. SARI

European Atomic Energy Community — EURATOM  
Joint Nuclear Research Center — Karlsruhe Establishment (Germany)  
European Transuranium Institute  
Luxembourg, February 1970 — 38 Pages — 14 Figures — FB 60

Sintered pellets of uranium-plutonium mixed oxides with  $\frac{Pu}{U + Pu}$  ratios from 5 to 90 % were oxidized under appropriate oxygen partial pressures at different temperatures. The oxidized samples were analyzed by ceramography and X-ray diffraction. The results were used to construct the partial U-Pu-O phase diagram for  $\frac{O}{U + Pu} \geq 2.00$  at room temperature, 600°, 1 000° and 1 400° C.

At room temperature a two phase region  $MO_{2+x} + "M_4O_9"$  was observed

---

## EUR 4136 e

STUDIES ON THE TERNARY SYSTEM  $UO_2-U_3O_8-PuO_2$   
by U. BENEDICT and C. SARI

European Atomic Energy Community — EURATOM  
Joint Nuclear Research Center — Karlsruhe Establishment (Germany)  
European Transuranium Institute  
Luxembourg, February 1970 — 38 Pages — 14 Figures — FB 60

Sintered pellets of uranium-plutonium mixed oxides with  $\frac{Pu}{U + Pu}$  ratios from 5 to 90 % were oxidized under appropriate oxygen partial pressures at different temperatures. The oxidized samples were analyzed by ceramography and X-ray diffraction. The results were used to construct the partial U-Pu-O phase diagram for  $\frac{O}{U + Pu} \geq 2.00$  at room temperature, 600°, 1 000° and 1 400° C.

At room temperature a two phase region  $MO_{2+x} + "M_4O_9"$  was observed

---

## EUR 4136 e

STUDIES ON THE TERNARY SYSTEM  $UO_2-U_3O_8-PuO_2$   
by U. BENEDICT and C. SARI

European Atomic Energy Community — EURATOM  
Joint Nuclear Research Center — Karlsruhe Establishment (Germany)  
European Transuranium Institute  
Luxembourg, February 1970 — 38 Pages — 14 Figures — FB 60

Sintered pellets of uranium-plutonium mixed oxides with  $\frac{Pu}{U + Pu}$  ratios from 5 to 90 % were oxidized under appropriate oxygen partial pressures at different temperatures. The oxidized samples were analyzed by ceramography and X-ray diffraction. The results were used to construct the partial U-Pu-O phase diagram for  $\frac{O}{U + Pu} \geq 2.00$  at room temperature, 600°, 1 000° and 1 400° C.

At room temperature a two phase region  $MO_{2+x} + "M_4O_9"$  was observed

---

with  $\frac{O}{M}$  up to 2.20 and  $\frac{Pu}{U + Pu} \leq 0.30$ . A single phase "M<sub>4</sub>O<sub>9</sub>" type exists with  $\frac{O}{M}$  between 2.20 and 2.27. This phase does not show a superlattice as reported for U<sub>4</sub>O<sub>9</sub>. With increasing temperature the two phase region becomes smaller. At 1 400° C a single fluorite phase exists for all Pu concentrations and  $\frac{O}{M}$  up to 2.27.

Above O/M = 2.27 and for overall Pu/U + Pu ratios below 0.5, a plutonium-rich fluorite phase is in equilibrium with a uranium-rich orthorhombic U<sub>3</sub>O<sub>8</sub>-type phase. When oxidation takes place at 600° C a metastable phase of the tetragonal U<sub>3</sub>O<sub>7</sub> type is formed for  $\frac{Pu}{U + Pu} < 0.25$  and  $\frac{O}{M} \leq 2.28$ ; and no segregation of plutonium occurs between the U<sub>3</sub>O<sub>8</sub>-type phase and the fluorite phase, because cation diffusion is too slow at that temperature. The oxidation limit in air was determined for all compositions and temperatures studied. The pattern of the U<sub>3</sub>O<sub>8</sub> structure was completely indexed with reference to its pseudo-hexagonal form, and the dependence of its lattice parameters from oxygen and plutonium content was studied.

with  $\frac{O}{M}$  up to 2.20 and  $\frac{Pu}{U + Pu} \leq 0.30$ . A single phase "M<sub>4</sub>O<sub>9</sub>" type exists with  $\frac{O}{M}$  between 2.20 and 2.27. This phase does not show a superlattice as reported for U<sub>4</sub>O<sub>9</sub>. With increasing temperature the two phase region becomes smaller. At 1 400° C a single fluorite phase exists for all Pu concentrations and  $\frac{O}{M}$  up to 2.27.

Above O/M = 2.27 and for overall Pu/U + Pu ratios below 0.5, a plutonium-rich fluorite phase is in equilibrium with a uranium-rich orthorhombic U<sub>3</sub>O<sub>8</sub>-type phase. When oxidation takes place at 600° C a metastable phase of the tetragonal U<sub>3</sub>O<sub>7</sub> type is formed for  $\frac{Pu}{U + Pu} < 0.25$  and  $\frac{O}{M} \leq 2.28$ , and no segregation of plutonium occurs between the U<sub>3</sub>O<sub>8</sub>-type phase and the fluorite phase, because cation diffusion is too slow at that temperature. The oxidation limit in air was determined for all compositions and temperatures studied. The pattern of the U<sub>3</sub>O<sub>8</sub> structure was completely indexed with reference to its pseudo-hexagonal form, and the dependence of its lattice parameters from oxygen and plutonium content was studied.

with  $\frac{O}{M}$  up to 2.20 and  $\frac{Pu}{U + Pu} \leq 0.30$ . A single phase "M<sub>4</sub>O<sub>9</sub>" type exists with  $\frac{O}{M}$  between 2.20 and 2.27. This phase does not show a superlattice as reported for U<sub>4</sub>O<sub>9</sub>. With increasing temperature the two phase region becomes smaller. At 1 400° C a single fluorite phase exists for all Pu concentrations and  $\frac{O}{M}$  up to 2.27.

Above O/M = 2.27 and for overall Pu/U + Pu ratios below 0.5, a plutonium-rich fluorite phase is in equilibrium with a uranium-rich orthorhombic U<sub>3</sub>O<sub>8</sub>-type phase. When oxidation takes place at 600° C a metastable phase of the tetragonal U<sub>3</sub>O<sub>7</sub> type is formed for  $\frac{Pu}{U + Pu} < 0.25$  and  $\frac{O}{M} \leq 2.28$ , and no segregation of plutonium occurs between the U<sub>3</sub>O<sub>8</sub>-type phase and the fluorite phase, because cation diffusion is too slow at that temperature. The oxidation limit in air was determined for all compositions and temperatures studied. The pattern of the U<sub>3</sub>O<sub>8</sub> structure was completely indexed with reference to its pseudo-hexagonal form, and the dependence of its lattice parameters from oxygen and plutonium content was studied.

**EUR 4136 e**

EUROPEAN ATOMIC ENERGY COMMUNITY — EURATOM

**STUDIES ON THE TERNARY SYSTEM  $\text{UO}_2$  -  $\text{U}_3\text{O}_8$  -  $\text{PuO}_2$**

by

U. BENEDICT and C. SARI

1970



Joint Nuclear Research Center  
Karlsruhe Establishment — Germany

European Transuranium Institute

## ABSTRACT

Sintered pellets of uranium-plutonium mixed oxides with  $\frac{\text{Pu}}{\text{U} + \text{Pu}}$  ratios from 5 to 90 % were oxidized under appropriate oxygen partial pressures at different temperatures. The oxidized samples were analyzed by ceramography and X-ray diffraction. The results were used to construct the partial U-Pu-O phase diagram for  $\frac{\text{O}}{\text{U} + \text{Pu}} \geq 2.00$  at room temperature, 600°, 1 000° and 1 400° C.

At room temperature a two phase region  $\text{MO}_{2+x} + \text{''M}_4\text{O}_9\text{''}$  was observed with  $\frac{\text{O}}{\text{M}}$  up to 2.20 and  $\frac{\text{Pu}}{\text{U} + \text{Pu}} \leq 0.30$ . A single phase "M<sub>4</sub>O<sub>9</sub>" type exists with  $\frac{\text{O}}{\text{M}}$  between 2.20 and 2.27. This phase does not show a superlattice as reported for U<sub>4</sub>O<sub>9</sub>. With increasing temperature the two phase region becomes smaller. At 1 400° C a single fluorite phase exists for all Pu concentrations and  $\frac{\text{O}}{\text{M}}$  up to 2.27.

Above O/M = 2.27 and for overall Pu/U + Pu ratios below 0.5, a plutonium-rich fluorite phase is in equilibrium with a uranium-rich orthorhombic U<sub>3</sub>O<sub>8</sub>-type phase. When oxidation takes place at 600° C a metastable phase of the tetragonal U<sub>3</sub>O<sub>7</sub> type is formed for  $\frac{\text{Pu}}{\text{U} + \text{Pu}} < 0.25$  and  $\frac{\text{O}}{\text{M}} \leq 2.28$ , and no segregation of plutonium occurs between the U<sub>3</sub>O<sub>8</sub>-type phase and the fluorite phase, because cation diffusion is too slow at that temperature.

The oxidation limit in air was determined for all compositions and temperatures studied. The pattern of the U<sub>3</sub>O<sub>8</sub> structure was completely indexed with reference to its pseudohexagonal form, and the dependence of its lattice parameters from oxygen and plutonium content was studied.

## KEYWORDS

URANIUM DIOXIDE  
U 3 O 8  
PLUTONIUM OXIDES  
SINTERED MATERIALS  
PELLETS  
CERAMICS  
X RADIATION  
DIFFRACTION  
PHASE DIAGRAMS  
HIGH TEMPERATURE  
METALLOGRAPHY  
STOICHIOMETRY  
URANIUM OXIDES

Contents

Introduction

1. Experimental

- 1.1. Preparation of the starting material
- 1.2. Oxidation of samples
- 1.3. X-ray measurements
- 1.4. Metallography

2. Results

- 2.1. Phase diagram at room temperature
- 2.2. Plutonium segregation at 1000°C
- 2.3. Phase diagram at 1400°C
- 2.4. Metastable phase diagram at 600°C
- 2.5. Oxidation limit in air
- 2.6. Tie-lines in the  $M'_3O_{8-z} + M''O_{2+x}$  phase field
- 2.7. The structure of the  $U_3O_8$  type phase

3. Discussion

-----





# STUDIES ON THE TERNARY SYSTEM $UO_2 - U_3O_8 - PuO_2$ \*)

---

## Introduction

The U-Pu-O system has been studied by several authors, using mainly high temperature and room temperature X-ray methods. BRETT and FOX investigated the oxidation behaviour of U-Pu mixed oxides at 750°C (4). DEAN made X-ray measurements on mixed oxides at 800° - 1400°C (3). These data have been used by MARKIN and STREET (1) (2), together with their own X-ray measurements, to construct a tentative partial U-Pu-O phase diagram. Preliminary results on the U-Pu-O system at 600° and 1000°C have been communicated by SARI, BENEDICT and BLANK (5).

As the results presented up to now were rather incomplete, we have undertaken more detailed studies, using micrographic and X-ray analysis.

-----

---

\*) Manuscript received on 14 May 1969.

## 1. Experimental

### 1.1. Preparation of the starting material

The starting material used was sintered pellets of general composition  $U_{1-y}Pu_yO_2$ , with  $y = \frac{Pu}{U+Pu}$ .

These were obtained by coprecipitating ammonium diuranate and plutonium hydroxide from a nitrate solution, calcining in air, reducing in hydrogen, compacting to pellets and sintering in a  $N_2/8\%H_2$  mixture at  $1500^\circ - 1700^\circ C$ . The U/Pu ratio and impurities of each batch was determined by chemical analysis. A typical impurity analysis is given in table I. Homogeneity was ascertained by autoradiography, metallography and X-ray diffraction. The oxygen stoichiometry was determined gravimetrically by equilibration of duplicate samples with a  $CO/CO_2$  10 : 1 mixture at  $850^\circ C$  (6) and from lattice parameter measurements.

### 1.2. Oxidation of samples

Small discs 2 - 3 mm thick were cut from the sintered pellets and oxidized under appropriate oxygen partial pressures at  $600^\circ$ ,  $1000^\circ$  and  $1400^\circ C$  and then quenched to  $3^\circ C$ . In order to determine the phase diagram at room temperature, a set of samples were oxidized at  $900^\circ C$  and cooled slowly to room temperature.

The O/M ratios of the oxidized specimens were determined by equilibration with a  $CO/CO_2$  10 : 1 mixture at  $850^\circ C$  (6).

### 1.3. X-ray measurements

Samples were studied in a 114.6 mm  $\emptyset$  Debye-Scherrer camera and on a Siemens diffractometer. These instruments had been con-

TABLE I

Typical impurity analysis of sintered (U,Pu)O<sub>2</sub> pellets

	<u>ppm</u>
Fe	< 50
Si	100
Mg	20
Mn	< 10
Cr	5
Ni	< 10
Pb	not detected
Bi	not detected
Al	< 100
Mo	< 10
Sn	not detected
Ag	2
Zn	not detected
Cd	not detected
V	not detected

structured or modified for use with Pu (7). For Debye-Scherrer work, Ni-filtered CuK-radiation was used. With the diffractometer, pure  $\text{CuK}\alpha_1$  diffraction diagrams were obtained by inserting a quartz monochromator between the sample and the counter tube. Cubic lattice parameters were obtained by extrapolation against  $\cos^2\theta$  wherever sharp high angle lines were available. In the other cases, lattice parameters were obtained from d-values suitably corrected for systematic errors.

#### 1.4. Metallography

The samples were cut, cold-mounted in araldite, ground on 600 emery paper and polished with 3, 1 and 1/4 micron diamond paste on microcloth. The microstructure was revealed by chemical etching with a variety of etchants consisting mainly of  $\text{HNO}_3$ ,  $\text{H}_2\text{SO}_4$ , HF and  $\text{H}_2\text{O}_2$  in varying proportions chosen according to the Pu and O contents of the sample.

## 2. Results

### 2.1. Phase diagram at room temperature

$(\text{U,Pu})\text{O}_2$  solid solutions were oxidized at  $900^\circ\text{C}$  under appropriate oxygen partial pressures for 20 hrs. and cooled down slowly to room temperature. The results of ceramographic and X-ray analysis are represented in the phase diagram of fig. 1.

A two phase region containing two fluorite phases has been found for  $0 < y \leq 0.30$ ; the high and low oxygen limits of this region vary with the plutonium content (see fig. 1). The phases have been designated  $\text{MO}_{2+x}$  and " $\text{M}_4\text{O}_9$ ". Typical microstructures of this region are shown in fig. 3 and compared with those found in the U-O systems, fig. 2. On the basis of

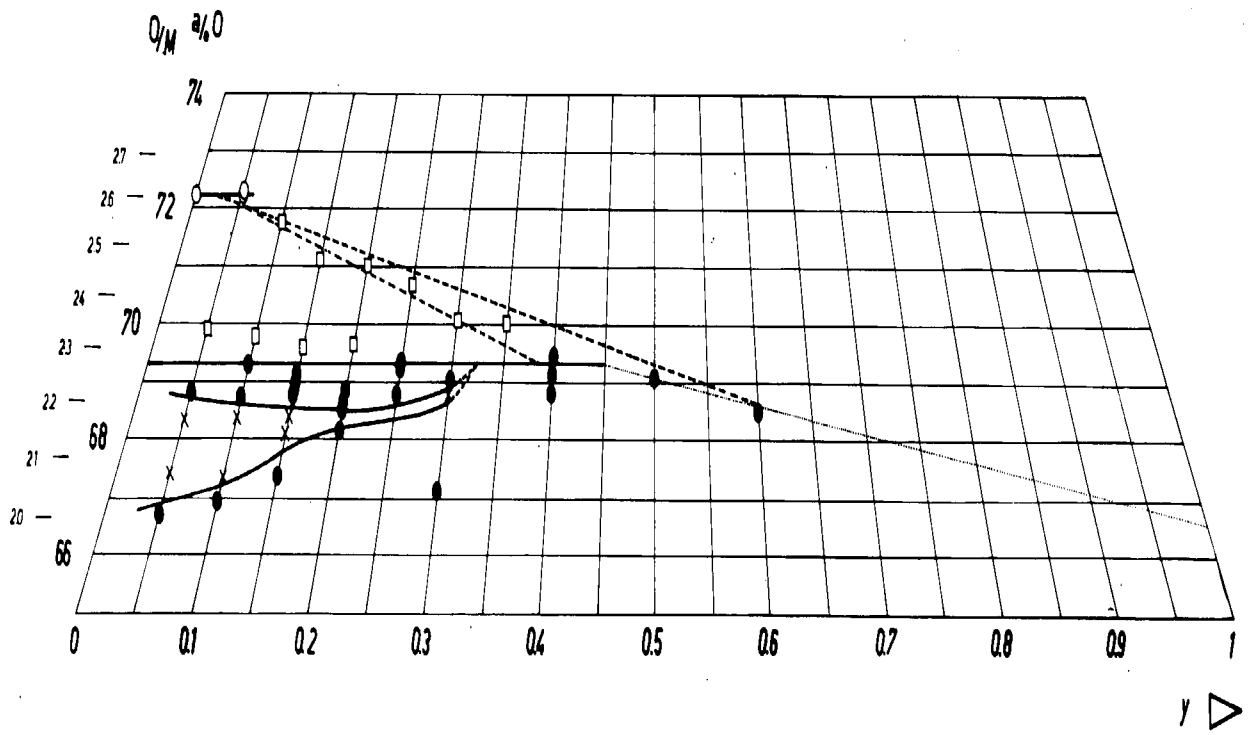
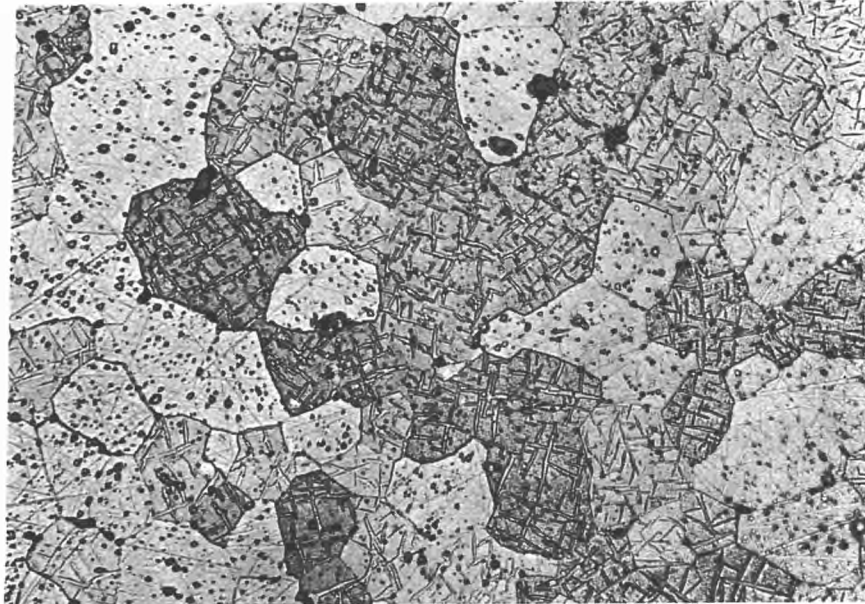


Fig. 1 Phase diagram at room temperature



$UO_{2.06}$

x 500

Fig. 2 - Microstructure of two phase region  $UO_{2+x} + U_4O_9$   
at room temperature

the similarity of the micrographs, figs. 2 and 3, the single phase with  $2.20 \leq \frac{O}{M} = 2.27$  and  $\frac{Pu}{U+Pu} \leq 0.30$  was named "M<sub>4</sub>O<sub>9</sub>" (fig. 4) although no superlattice of the U<sub>4</sub>O<sub>9</sub> type has been detected by X-rays. The X-ray results given in table II confirm the existence of a two phases region. The oxygen content and the ratio of the two FCC phase as determined by X-ray line intensities were used to draw the limits of the region. We believe that at  $y \simeq 0.30$  the "M<sub>4</sub>O<sub>9</sub>" type phase transforms into a normal FCC phase.

A two phase region exists for  $\frac{O}{M}$  between 2.28 and 2.61 and extends into the diagram up to about U<sub>0.5</sub>Pu<sub>0.5</sub>O<sub>2.25</sub>. A typical microstructure is shown in fig. 5. The two phases are a uranium-rich U<sub>3</sub>O<sub>8</sub>-type phase designated M<sub>3</sub>O<sub>8-z</sub>, and a plutonium-rich MO<sub>2+x</sub> fluorite type phase. From the M<sub>3</sub>O<sub>8</sub> single phase field at  $\frac{O}{M} > 2.61$  it can be seen that the solubility of Pu in U<sub>3</sub>O<sub>8</sub> ends at  $y \sim 0.06$ . So any point in the above mentioned two phase region is situated on a tie-line joining a point on the low oxygen limit of the MO<sub>2+x</sub> phase field. The compositions of the end points of the tie-line are designated by M'<sub>3</sub>O<sub>8-z</sub> and M''O<sub>2+x</sub>, respectively. The method used for the determination of the tie-lines will be described in sect. 2.6. The dotted line joining U<sub>0.5</sub>Pu<sub>0.5</sub>O<sub>2.25</sub> and PuO<sub>2</sub> represents the oxidation limit at 900° in air and not necessarily a phase boundary. For the same reason, the M'<sub>3</sub>O<sub>8-z</sub> + M''O<sub>2+x</sub> region has not been completely delimited to high oxygen contents.

## 2.2. Plutonium segregation at 1000°C

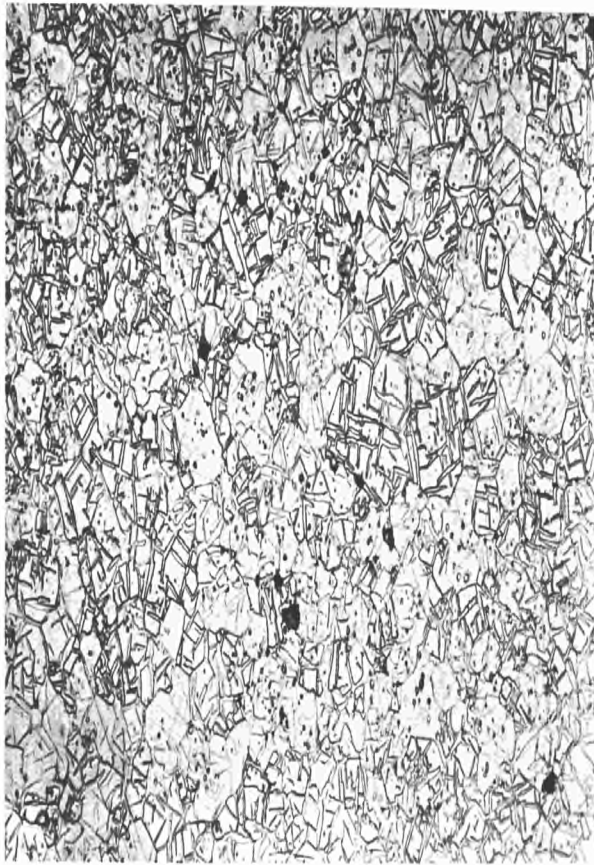
The (U,Pu)O<sub>2</sub> pellets were oxidized at 1000°C for 20 hrs to the desired  $\frac{O}{M}$  ratio and then quenched. The main purpose was to investigate the plutonium migration in the region of high O/M ratio. A rough estimation of plutonium diffusion in MO<sub>2+x</sub> had already been made on the basis of metallographic results (5). The experimental results are represented in fig 6 and 7.

y	O/M	low oxygen f.c.c. phase		high oxygen f.c.c. phase	
		a [ $\text{\AA}$ ]	amount [%]	a [ $\text{\AA}$ ]	amount [%]
0.05	2.218	-	-	5.4395	100
0.10	2.208	-	-	5.4395	100
0.15	2.07	5.4535	100		
0.15	2.14	5.4509 <sup>2</sup>	60	5.4344 <sup>2</sup>	40
	2.17	5.4506 <sup>3</sup>	41	5.4332 <sup>2</sup>	59
	2.21	-	-	5.4324	100
	2.23	-	-	5.4286	100
0.20	2.15	5.4373	100	-	-
	2, 19	-	-	5.4329	100
	2.22	-	-	5.4243	100
0.25	2.26	-	-	5.4259	100
0.30	2.21	5.4294 <sup>1</sup>	45	5.4225 <sup>1</sup>	55
	2.24	-	-	5.4210	100

Table II

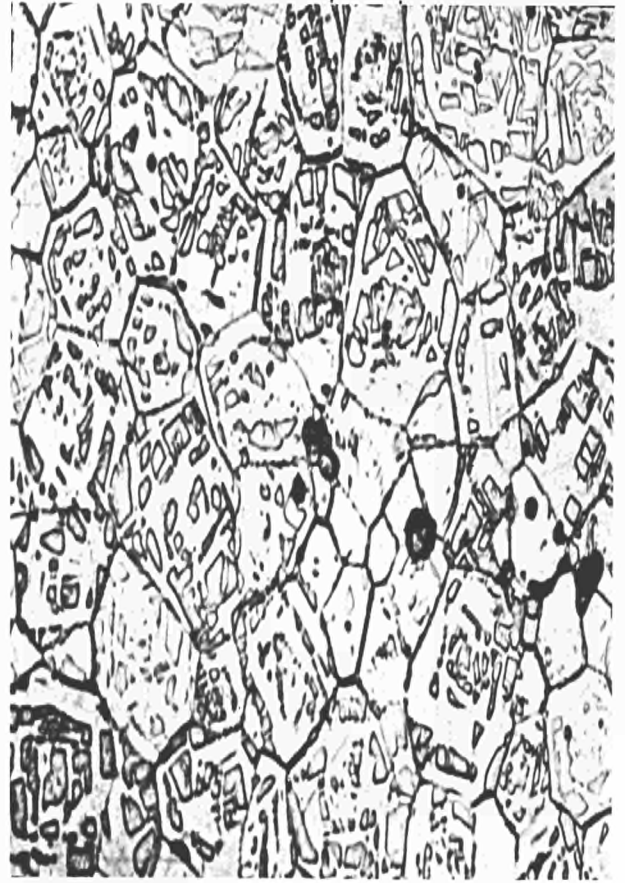
Lattice parameters of f.c.c. phases for samples slowly cooled from 900 - 1000°C. Errors are in general  $\pm 0.0005 \text{ \AA}$ . Larger errors are indicated by superscripts: <sup>1</sup> =  $\pm 0.001 \text{ \AA}$ , <sup>2</sup> =  $\pm 0.002 \text{ \AA}$ ; <sup>3</sup> =  $\pm 0.003 \text{ \AA}$ .





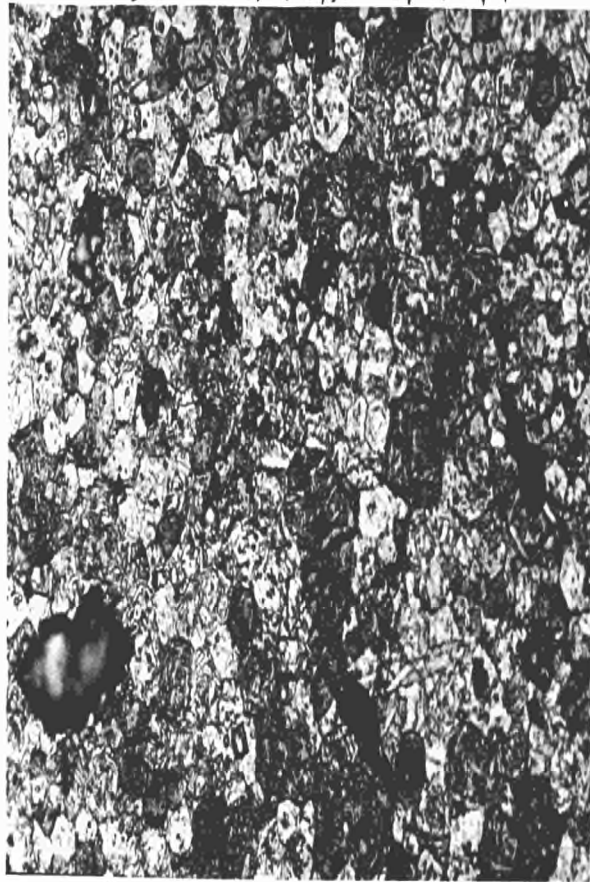
a)  $(U_{0,95}Pu_{0,05})O_{2,08}$

x 500



b)  $(U_{0,90}Pu_{0,10})O_{2,17}$

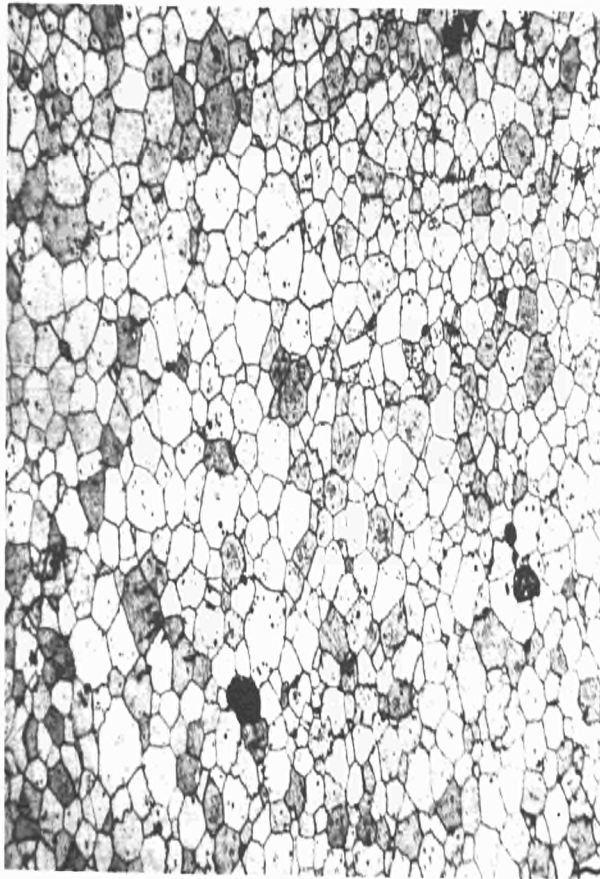
x 1000



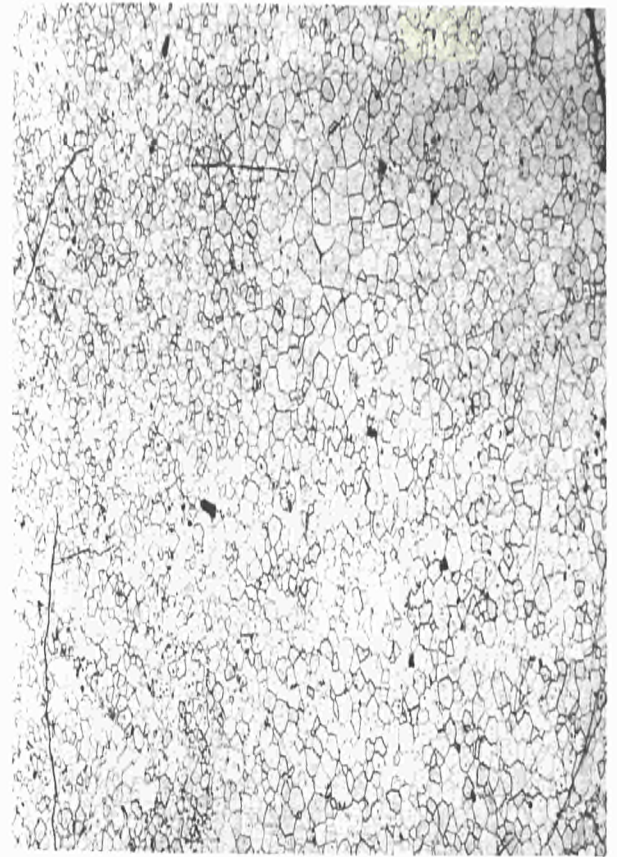
c)  $(U_{0,85}Pu_{0,15})O_{2,14}$

x 500

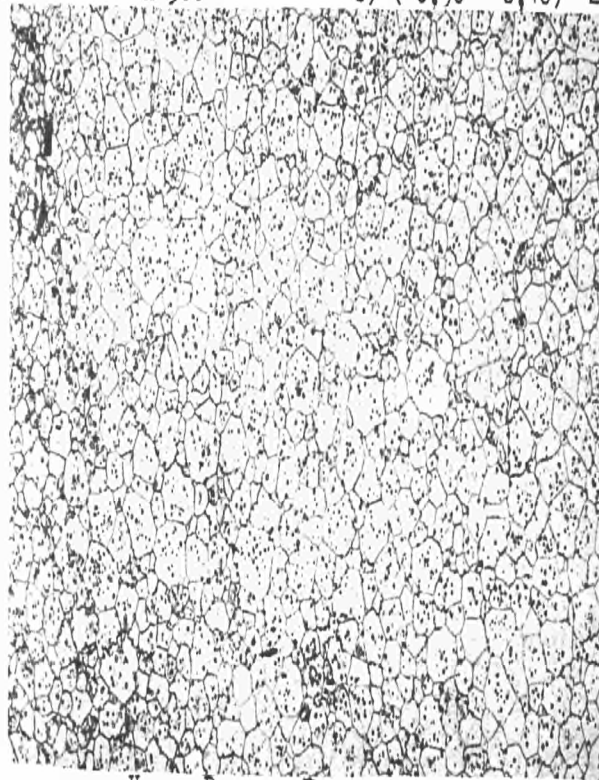
Fig. 3 - Microstructure of two phase region  $MO_{2+x} + "M_4O_9"$  at room temperature.



a)  $(U_{0.95}Pu_{0.05})O_{2.218}$  x 500

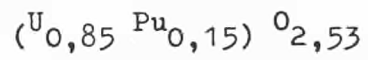
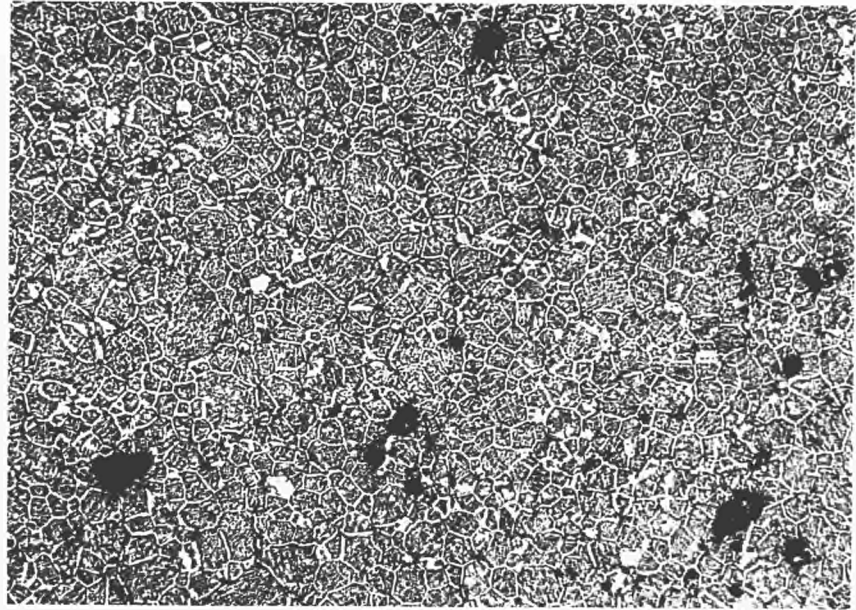


b)  $(U_{0.90}Pu_{0.10})O_{2.208}$  x 200



c)  $(U_{0.85}Pu_{0.15})O_{2.23}$  x 500

Fig. 4 - Microstructure of the " $M_4O_9$ " type single phase at room temperature.



x 200

Fig. 5 - Microstructure of two phase region  $\text{M}'_3\text{O}_{8-z} + \text{M}''\text{O}_{2+x}$   
at room temperature

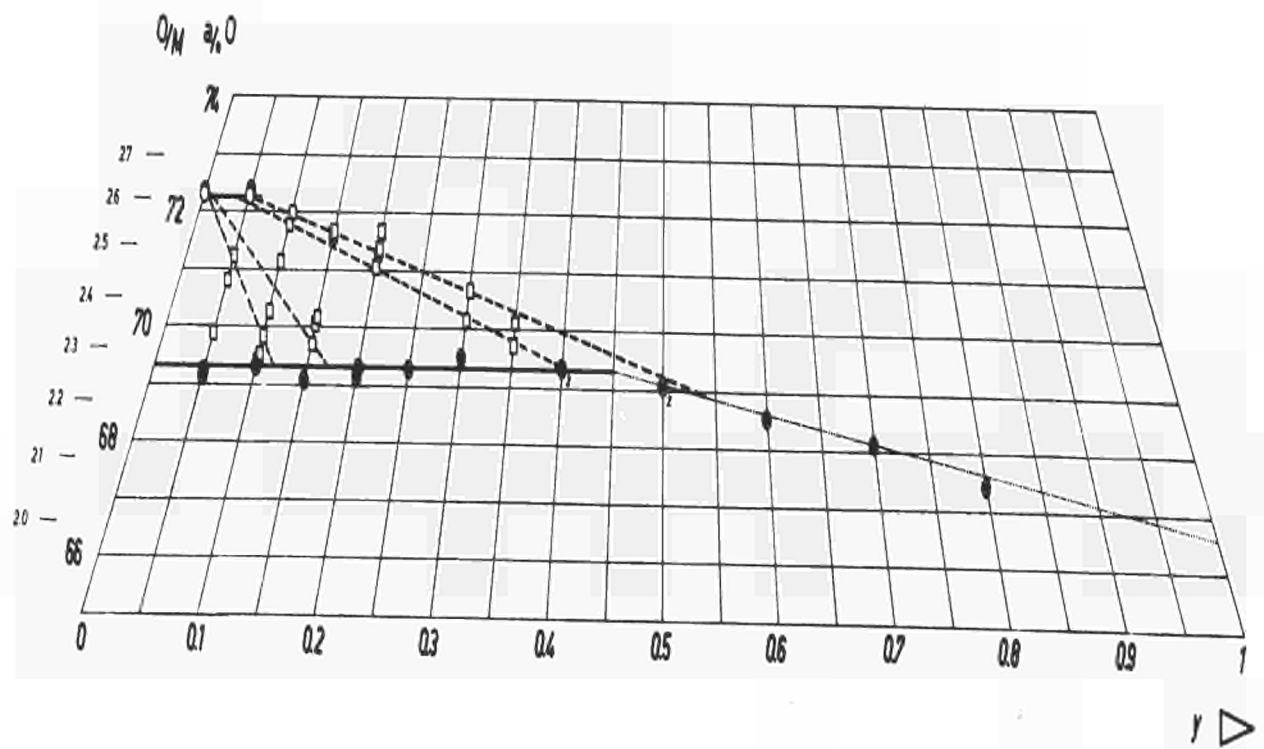
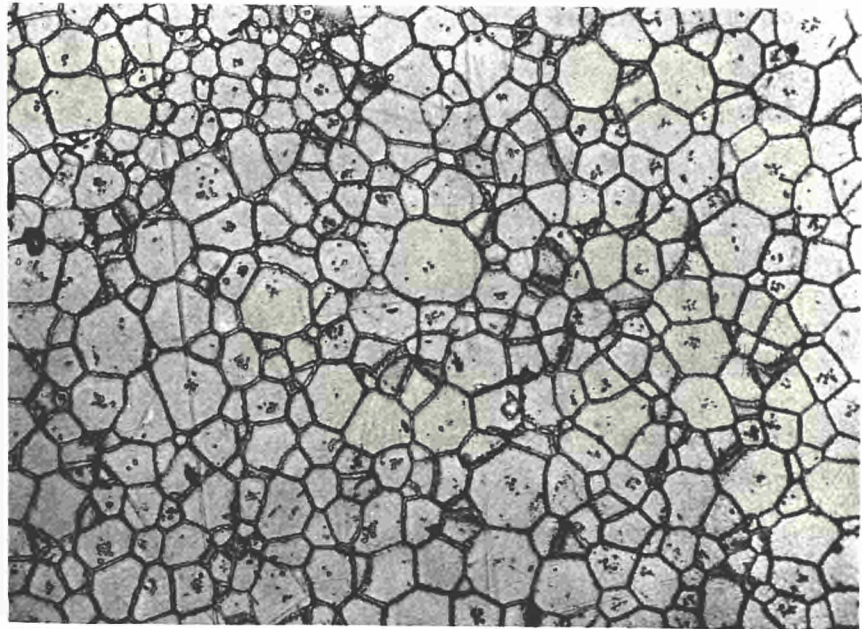


Fig. 6 Orthorhombic + cubic two phase region at 1000° C



x 500

$(U_{0,90} Pu_{0,10}) O_{2,32}$ . Orthorhombic  $M'_{3}O_{8-z}$   
precipitates at the grain boundaries of the  
 $M''O_{2+x}$  matrix

Fig. 7 - Microstructure of two phase specimens at 1000° C

Like in the room temperature phase diagram, no superstructure lines corresponding to the  $U_4O_9$  structure type were found in the region around  $MO_{2.25}$ .

The  $M'_3O_{8-z} + M''O_{2+x}$  region at  $1000^\circ C$  is very similar to that observed after slowly cooling at room temperature; the maximum Pu content of the  $M_3O_8$  phase is about  $y = 0.06$  and the tie-lines behave similarly (see sect. 2.6.). The lines limiting the diagram towards high oxygen contents are no phase boundaries, but lines of maximum oxidation in air (see sect. 2.5.).

### 2.3. Phase diagram at $1400^\circ C$

Samples were oxidized at  $1400^\circ C$  for 6 - 20 hrs and quenched. The phase diagram for the regions studied is given in fig. 8. Qualitatively it shows the same phase fields as that for  $1000^\circ C$ . Examples of the microstructures are shown in fig. 9 and 10.

We did not succeed in preparing single phase  $M_3O_8$ , because its dissociation pressure at  $1400^\circ C$  is higher than the oxygen partial pressure in air. So we could not directly determine the solubility of plutonium in  $U_3O_8$  at  $1400^\circ C$ . But from the study of the tie-lines in the  $M'_3O_{8-z} + M''O_{2+x}$  field, a maximum solubility of about 2 % Pu can be deduced for our experimental conditions. Similarly, the oxidation limit of the two phase specimens at  $1400^\circ C$  is lower than at  $1000^\circ C$ , so the region studied is somewhat smaller.

### 2.4. Metastable phase diagram at $600^\circ C$

The samples were oxidized at  $600^\circ C$  in an atmosphere of appropriate oxygen partial pressure for 20 to 30 hrs and quenched. The results are given in fig. 11.

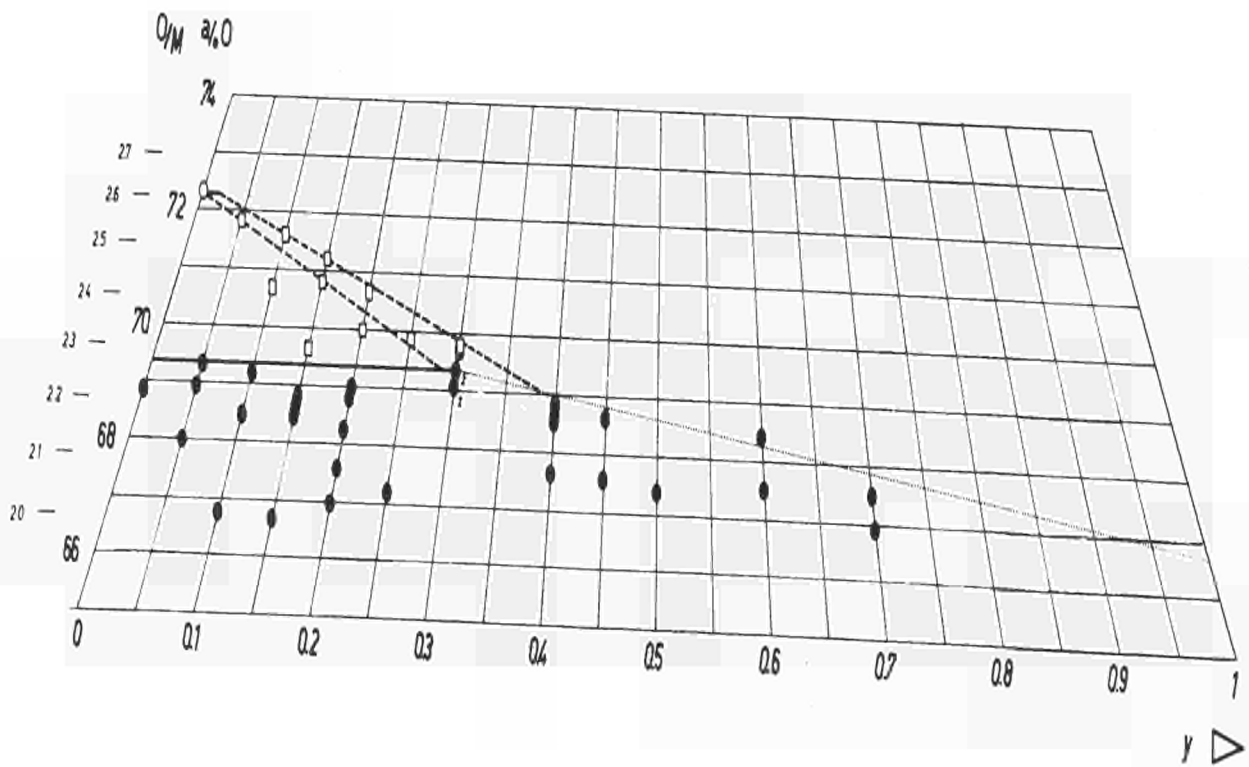
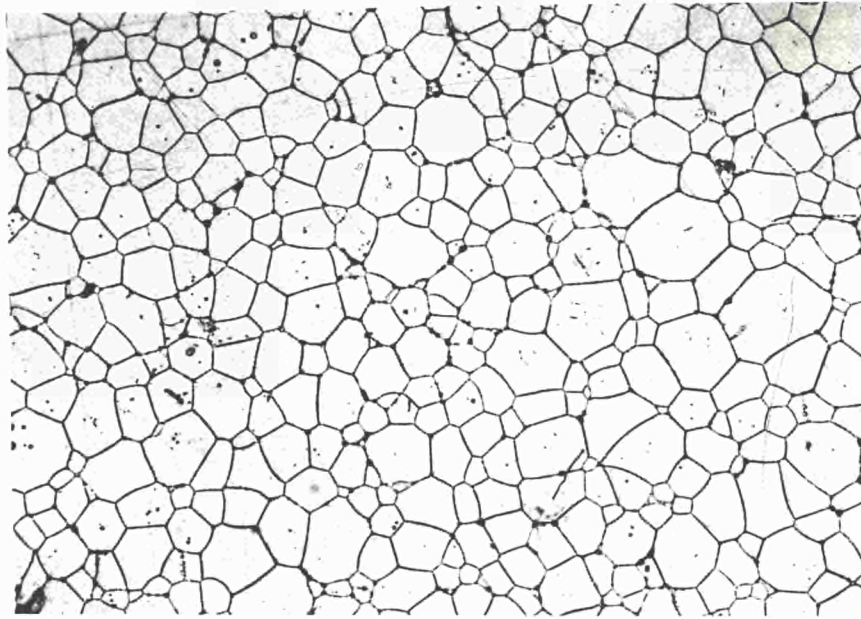
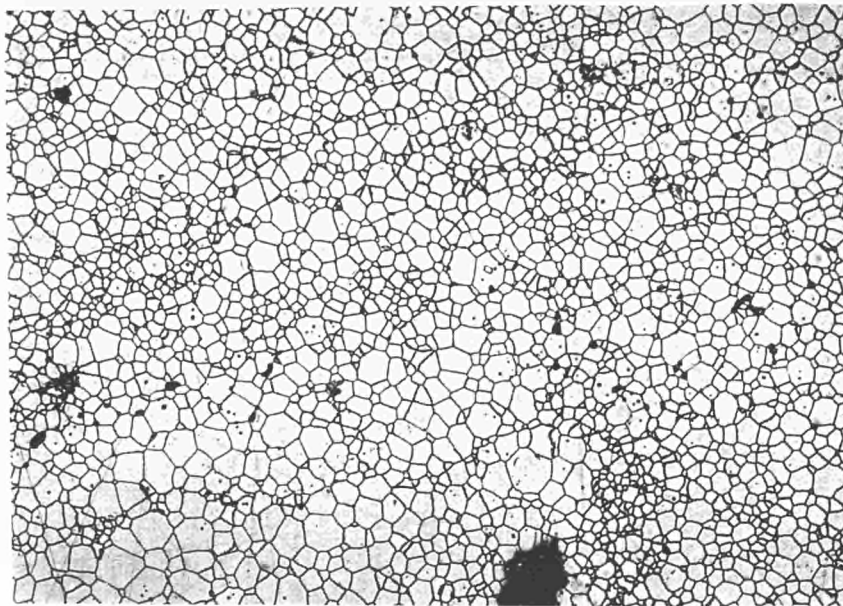


Fig. 8 - Phase diagram at 1400 ° C



x 500

a)  $(U_{0,70} Pu_{0,30}) O_{2,24}$ . Single phase  $MO_{2+x}$

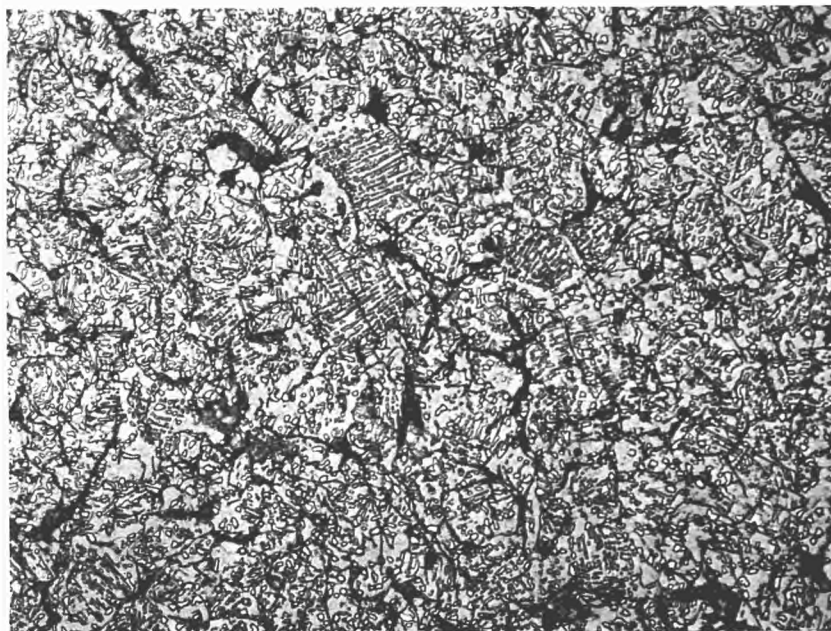


x 200

b)  $(U_{0,90} Pu_{0,10}) O_{2,27}$ . Single phase  $MO_{2+x}$

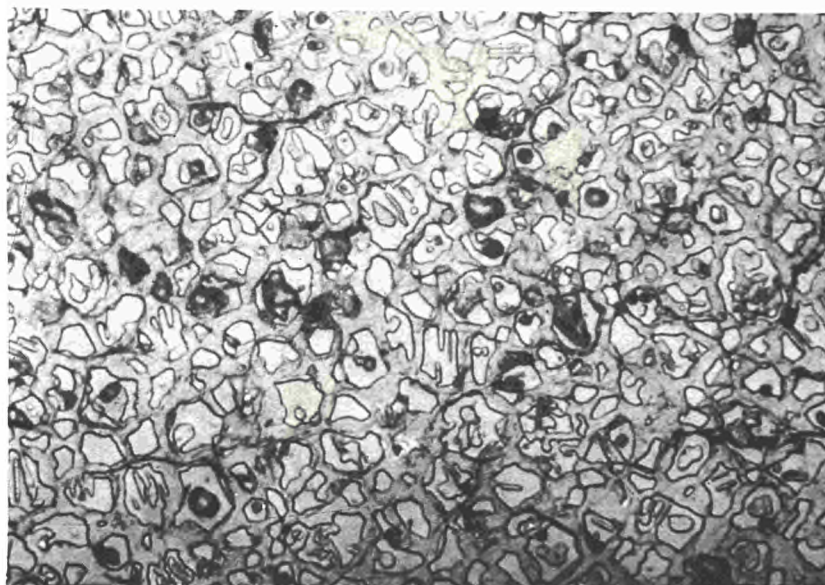
Fig. 9 - Microstructure of the f.c.c.  $MO_{2+x}$  phase at 1400° C





a) (U<sub>0,95</sub> Pu<sub>0,05</sub>) O<sub>2,54</sub>

x 500



b) (U<sub>0,80</sub> Pu<sub>0,20</sub>) O<sub>2,42</sub>

x 1000

Fig. 10 - Microstructure of two phase region  $M'_{3}O_{8-z} + M''O_{2+x}$  at 1400° C

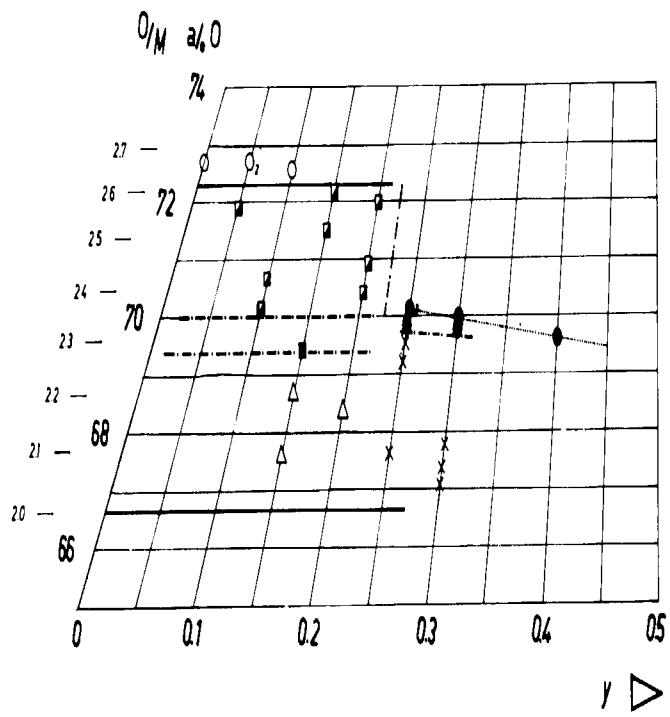


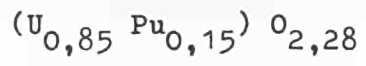
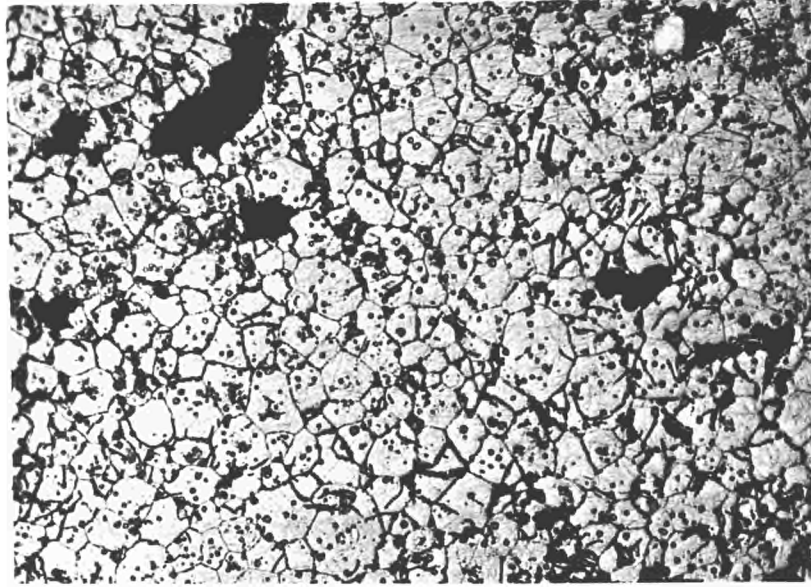
Fig. 11 - Metastable phase diagram at 600° C

This phase diagram differs from the other ones described above mainly by two points :

- 1) A tetragonal phase of the  $U_3O_7$  type, called consequently  $M_3O_7$ , replaces the cubic phases coexisting with  $M'_3O_{8-z}$  at the three temperatures discussed before and with  $MO_{2+x_1}$  at room temperature.
- 2) In the two phase field  $M_3O_{8-z} + M_3O_7$ , the two phases have the same plutonium content.

Samples oxidized at higher temperatures, cooled to  $600^\circ C$ , kept at this temperature for 6 hrs and then quenched, did not show a tetragonal phase. So it must be concluded that  $M_3O_7$  is a metastable phase. The tetragonal phase was observed together with  $MO_{2.00}$  at  $O/M \leq 2.20$ , as a single phase at  $O/M$  ratios between 2.27 and 2.28 (see fig. 12) and together with  $M_3O_{8-z}$  at  $O/M \geq 2.35$ . In the two phase samples it had lattice parameters  $a \sim 5.39$ ,  $c \sim 5.54$ , with  $c/a$  ratios from 1.028 to 1.031. This fits the data of  $\gamma_1-U_3O_7$  as named by PERIO (8), a variety which has been described by many workers (see ref. 9 for a recent review). So it has to be concluded that up to 20 % of the U atoms of  $U_3O_7$  can be replaced by Pu without noticeable change in lattice dimensions. In the two single phase samples observed, the tetragonal phase had  $c/a = 1.013$  and  $c/a = 1.008$ , resp. with  $a \sim 5.405$  in the two cases. These  $c/a$  ratios approximate that given for  $\gamma_3-U_3O_7$  by PERIO (8).

For  $y = 0.25$  no  $M_3O_7$  phase was found, but a single f.c.c. phase at  $O/M = 2.325$  and  $O/M = 2.357$ , and two coexisting f.c.c. phases for lower  $O/M$  ratios. The corresponding lattice parameters are reported in table III.



x 500

Fig. 12 - Microstructure of the  $\text{M}_3\text{O}_7$  single phase at 600°C

O/M	f.c.c. <sub>1</sub>	f.c.c. <sub>2</sub>
2.26	5.4255 ± 0.0005	5.4527 ± 0.0010
2.29	5.4260 ± 0.0005	5.4534 ± 0.0005
2.325	5.4256 ± 0.0005	
2.357	5.4247 ± 0.0005	

Table III

f.c.c. lattice parameters at  $y = 0.25$  for samples oxidized at 600 °C.

The four samples of table III constitute an internally coherent set of values. In fact, the lower parameters of the two phase samples approximate the parameter of the single phase sample with the lower O/M ratio. So we must conclude that the lower limiting O/M ratio of the single phase region is 2.32. The higher parameter of the two phase samples corresponds approximately to  $U_{0.75}Pu_{0.25}O_{2.00}$ . So for  $y = 0.25$  we have the same situation as for lower Pu contents with the exception that the tetragonal phase is replaced by a cubic phase of about the same O/M.

Also for  $y = 0.3$  and  $y = 0.4$  we found two f.c.c. phases at lower oxygen contents and one f.c.c. phase at O/M 2.30, but a rather large dispersion of lattice parameter values did not allow us to fix the phase limits in this region.

Single phase  $M_3O_8$  could be obtained only for  $y$  up to 0.10 with the air oxidation treatment. At  $y = 0.15$  and  $y = 0.2$ ,  $M_3O_{8-z}$  was obtained only in two phase samples. For  $y = 0.25$ , no  $M_3O_8$  phase was formed by oxidation in air. The  $M_3O_8$  single phase

region has been drawn to at least  $y = 0.2$ , as no noticeable cation diffusion takes place at  $600^{\circ}\text{C}$ , and so in the two phase samples with  $y = 0.2$  no Pu depletion of the  $\text{M}_3\text{O}_{8-z}$  occurs.

#### 2.5. Oxidation limit in air

Samples with Pu content  $y$  between 0.05 and 0.9 have been completely oxidized in air for 20 hrs at  $600^{\circ}$ ,  $1000^{\circ}$ , and  $1400^{\circ}\text{C}$ . Only pellets, no powders were used for oxidation in this experiment. The O/M ratio of the oxidation limit decreases with increasing temperature. The dotted lines drawn in the phase diagrams for the different temperatures represent the composition for which the dissociation pressure is equal to the oxygen partial pressure in air.

#### 2.6. Tie-lines in the $\text{M}'_3\text{O}_{8-z} + \text{M}''\text{O}_{2+x}$ field

Four independent quantities have been combined to determine the tie-lines in the  $\text{M}'_3\text{O}_{8-z} + \text{M}''\text{O}_{2+x}$  phase field at room temperature,  $1000^{\circ}$  and  $1400^{\circ}\text{C}$ .  $\text{M}'$  means (U,Pu) with low Pu content  $y'$ ,  $\text{M}''$  means (U,Pu) with high Pu content  $y''$ .

The samples have been analyzed in the oxidized state as well as after having been reduced again to  $\text{O/M} = 2.00$ . This reduction performed at  $850^{\circ}\text{C}$  in  $\text{CO/CO}_2$  (6) leaves the cation concentrations unchanged, leading thus to 2 f.c.c. phases  $\text{M}'\text{O}_{2.00}$  and  $\text{M}''\text{O}_{2.00}$ .

Samples oxidized at  $600^{\circ}\text{C}$  and then reduced back to  $\text{O/M} = 2.00$  showed only one  $\text{MO}_{2.00}$  phase, thus indicating that no U-Pu segregation had occurred between the  $\text{M}_3\text{O}_8$  and  $\text{M}_3\text{O}_7$  phases. The four independent quantities are :

a) M'/M'' ratio: This has been determined from the ratios of diffraction line intensities of the two coexisting phases in the oxidized as well as in the  $M'O_{2.00} + M''O_{2.00}$  state. The average of these two determinations was used. Intensity ratios  $M'_3O_{8-z}/M''O_{2+x}$  were calibrated against mixtures of known  $U_3O_8/UO_{2+x}$  ratio. For  $M'O_{2.00} + M''O_{2.00}$  intensity ratios are assumed to be equal to M'/M'' ratios.

b) y': For  $M'_3O_{8-z}$ , y' has been obtained from the b/a ratio of this orthorhombic phase using suitable calibration curves that will be discussed in sect. 2.7.

c) y'': Vegard's law between  $UO_{2.00}$  and  $PuO_{2.00}$  was used for finding y'' from the lattice parameters of  $M''O_{2.00}$ .

d) O/M: This was measured gravimetrically in the usual way.

Theoretically two of these four independent values would be sufficient to construct the tie-line for a given specimen. But it was found that imprecisions on the four variables were too large to allow this to be done. So only samples where at least three variables agreed with each other were used to construct the tie-lines given in the phase diagrams. To keep the diagrams sufficiently clear, only some characteristic tie-lines are indicated. It is seen that the tie-lines for  $1400^\circ\text{C}$  extend from  $0 < y' \lesssim 0.02$  at the  $M'_3O_{8-z}$  side, to values mainly between  $y'' = 0.25$  and  $y'' = 0.45$  at the  $MO_{2+x}$  side, for overall Pu contents from  $y = 0.05$  to  $y = 0.4$  and rather high degrees of oxidation. The limiting concentration of Pu in  $M'_3O_{8-z}$  at  $1400^\circ\text{C}$  is thus found to occur at  $y \sim 0.02$ . In the same manner, the limiting concentration at  $1000^\circ\text{C}$  was determined as being  $y \sim 0.06$ . At both temperatures, a high degree of oxidation and a high Pu content make the tie-lines to higher Pu contents at their two end points and vice versa.

The tie-lines and limiting Pu concentration in  $U_3O_8$  at room temperature are very similar to those observed at  $1000^\circ C$ .

## 2.7. The structure of the $U_3O_8$ type phase

The structure of  $U_3O_8$  is usually described in orthorhombic coordinates with  $a \sim 6.7$ ,  $b \sim 11.9$ ,  $c \sim 4.15$  (10)(11)(12). A hexagonal structure has been found in some cases, as for example in the work of SIEGEL (13)(14) who gives a complete indexing of hexagonal  $U_3O_8$ . No completely indexed pattern of orthorhombic  $U_3O_8$  was available in the literature, and there is no definite agreement on its space group. So an orthorhombic indexing had to be found that fitted our experimental data.

It was observed that in  $M_3O_8$  patterns a number of line doublets merged progressively to broad single lines as experimental conditions varied. The pattern so obtained corresponded to the hexagonal pattern given by SIEGEL (13). So in our samples a continuous transition from true orthorhombic to nearly hexagonal patterns could be observed, analogous to the transition found by SIEGEL. As hexagonal lattices can be described in terms of orthorhombic co-ordinates, this transition provided the means to check possible orthorhombic Miller indices by the known hexagonal indices, using the transformation relations between hexagonal and orthohexagonal indices of the same lattice plane. The Miller indices thus obtained are given in table IV. Table V shows a typical example of our  $M_3O_8$  patterns.

Literature data and our own measurements indicate that in orthorhombic  $U_3O_8$  the lattice parameter  $a$  increases and the lattice parameter  $b$  decreases with decreasing O/U ratio. The relation between the ratio  $b/a$  and the oxygen content O/U is shown in fig. 13. The ratio  $b/a$  was chosen as it partly eliminates experimental errors existing in  $a$  and  $b$ . In our pluto-



HEX	OR	HEX	OR
001	001	004	004
110	130 200	332	392 602
111	131 201	114	134 204
002	002	601	0.12.1 661
300	060 330	413	(193) 463 533
301	061 331	304	064 334
220	260 400	224	264 404
221	261 401	522	0.12.2 ? 662
311	421 (171) 351	440 ?	4.12.0 ? 800
302	062 332	005	005
003	003	115 ?	135 ? 205 ?
222	262 402	414	(194) 464 534
410	(190) 460 530		
411	(191) 461 531		
303	063 333		
331	391 601		
412	(192) 462 532		
223	263 403		

Table IV Correspondance between Miller indices of hexagonal and orthorhombic  $U_3O_8$ . Indices between brackets were very rarely found in our samples. A question mark means that a line was found at that place, but its position deviated more than normally from theoretical position.

hkl	d [Å]	100 I/I <sub>0</sub>	
		Diffraktometer	Debye-Scherrer
001	4.147	90	84
130	3.416	100	100
200	3.381	45	60
131/201	2.637	96	98
002	2.076	36	34
060	1.978	17	32
330	1.957	18	26
061	1.785	24	42
331	1.772	81	87
260	1.706	12	16
400	1.688	8	12
261	1.578	14	19
401	1.564	8	11
421	1.511	3	-
062	1.4310	12	22
332	1.4240	10	22
003	1.3828	8	17
262	1.3184	8	16
402	1.3098	5	-
460/530	1.2818	19	34
191	1.2353	7	20
063	1.1333	6	22
333	1.1303	6	28
462	1.0927	4	24
601/532	1.0895	3	
263	1.0740	4	
403	1.0692	3	
004	1.0371	3	
134	0.9924	10	31
0.12.1	0.9616	2	
463/533	0.9407	4	
064	0.9187	5	
334	0.9167	4	31
264/662	0.8865	5	
005	0.8299	3	-
194	0.8093	4	-
534	0.8063	8	43

Table V Typical example of diffraction pattern of  $M_3O_8$ .  
Composition  $U_{0.95}Pu_{0.05}O_{2.62}$ , single phase.

2 θ and d are corrected with reference to gold used as an internal standard. Debye-Scherrer intensities are peak heights of photometric record.

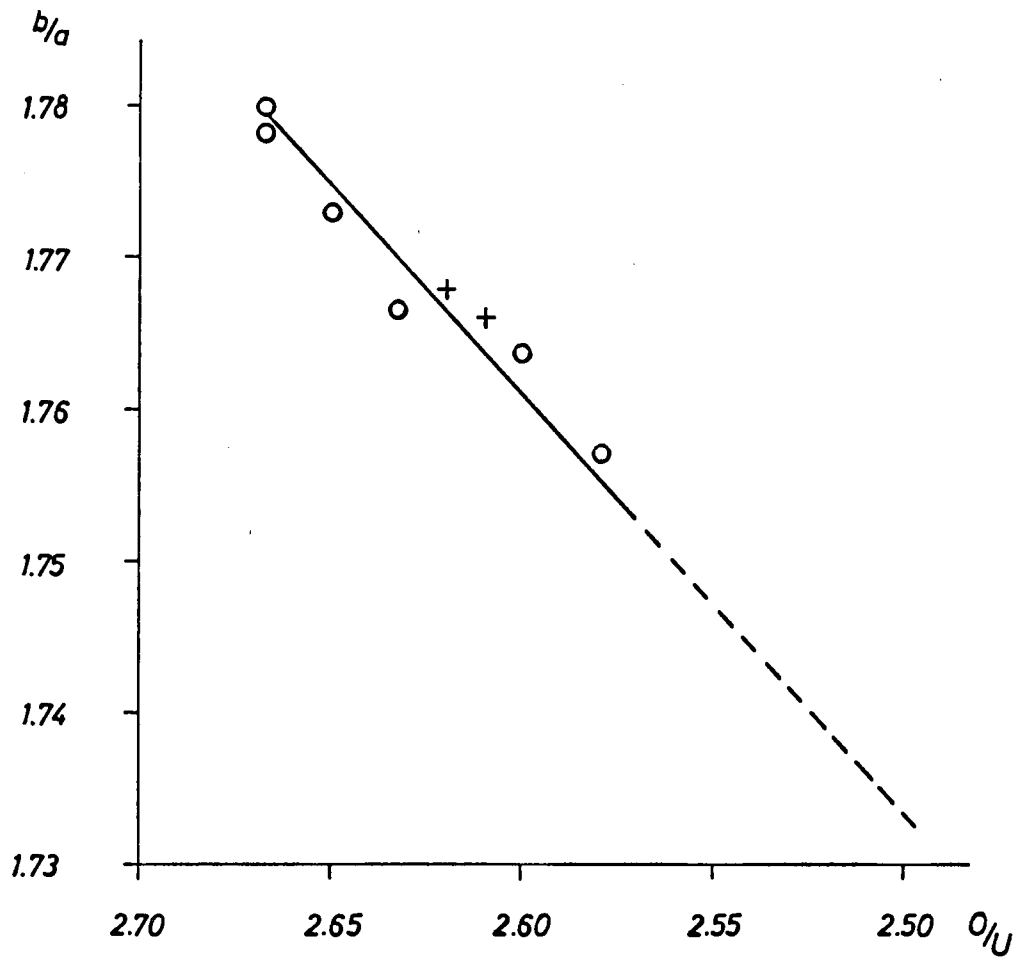


Fig. 13 - Orthorhombic  $b/a$  as a function of  $O/U$  in  $U_3O_8$  and  $M_3O_8$   
+ this work  
o literature data taken from the compilation of STEEB (15)

nium-containing samples, the variation of  $b/a$  is larger than could be expected from the differences in oxygen content measured. It has to be concluded that addition of Pu also makes  $b/a$  decrease, and that in our specimens both oxygen content and plutonium content contribute to the change in lattice dimensions. To separate them, the  $b/a$  ratios of  $M_3O_8$  phases with known Pu content were plotted against  $y$  (fig. 14). A straight line could be drawn with a good approximation, through the points representing the low oxygen limit of  $M_3O_{8-z}$ . As this limit has the same oxygen content for all Pu concentrations studied, the straight line of fig. 14 represented the variation of  $b/a$  with Pu content only. It has been used for determining  $y'$  from  $b/a$  in sect. 2.6.

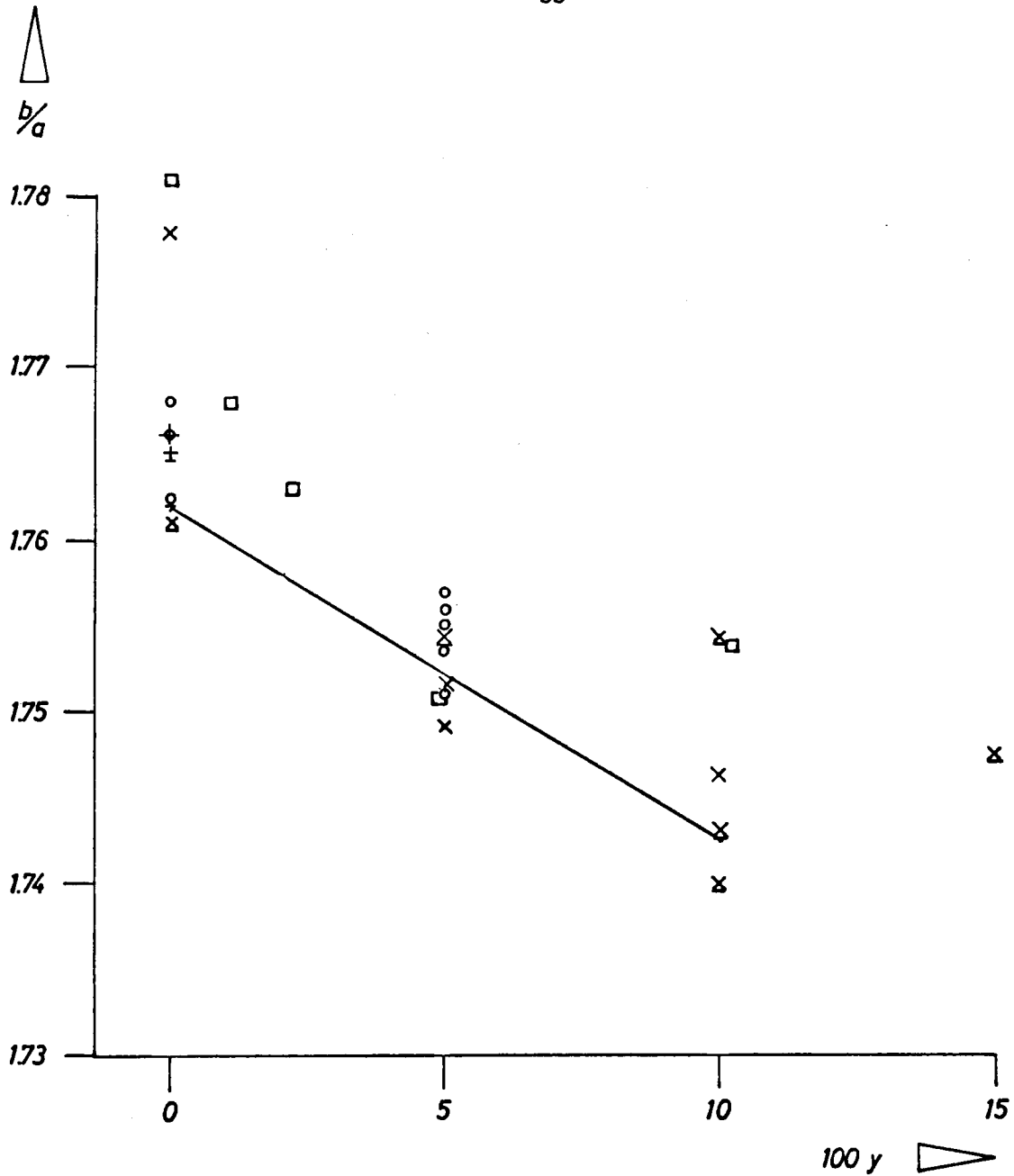


Fig. 14 - Orthorhombic  $b/a$  as a function of  $y$   
 x single phase samples, oxidized at  $600^{\circ} \text{C}$   
 o single phase samples, oxidized at  $1000^{\circ} \text{C}$   
 + single phase samples, oxidized at  $1400^{\circ} \text{C}$   
 single phase samples, oxidized at  $750^{\circ} \text{C}$  (4)

Underlined points correspond to  $\text{M}_3\text{O}_{8-z}$  coexisting with  $\text{MO}_{2+x}$  of the same Pu content and therefore represent the low oxygen limit of  $\text{M}_3\text{O}_{8-z}$ .

## Discussion

The phase diagrams proposed tentatively by MARKIN and STREET (1) (2) have been partially modified by this work. We found that at room temperature the single phase region " $M_4O_9$ " exists for low  $\frac{Pu}{U+Pu}$  ratio. Furthermore, the two phase region " $M_4O_9$ " has been enlarged in the direction of low  $\frac{O}{M}$  ratio and closed at about  $\frac{Pu}{U+Pu} = 0.32$ . It is unlikely that the " $M_4O_9$ " type phase exists for plutonium concentration much higher than 30 % as suggested (1).

Like MARKIN and STREET, we did not find any indication of a superlattice for the so-called " $M_4O_9$ " type phase. Therefore this phase cannot be crystallographically related to the  $U_4O_9$  which is considered an ordered type of the f.c.c.  $UO_{2+x}$  structure. On the other hand, the fact that  $U_4O_9$  and " $M_4O_9$ " precipitates are morphologically comparable as revealed by metallographic analysis, leads us to assume a close similarity between the U-Pu-O and the U- $\emptyset$  system, at least for  $\frac{Pu}{U+Pu} \leq 0.30$  and  $\frac{O}{M}$  up to 2.27. It is thought that " $M_4O_9$ " differs from  $MO_{2+x}$  but is not a completely ordered structure. The two phase region has been closed in the direction of high plutonium content with a dashed line only because of the difficulties to prepare suitable samples. It is nevertheless likely that it meets the phase boundary against the two phase field containing the cubic and the  $M_3O_{8-z}$  phase. The  $M_3O_{8-z}$  phase could be in equilibrium with " $M_4O_9$ " or  $MO_{2+x}$  according to the plutonium content.

The  $M_3O_8$  single phase region was given with its oxygen content decreasing with increasing Pu content, in the phase diagrams proposed earlier (1,2). Our results show that at least the low oxygen limit of this region remains constant with increasing Pu content. This is shown by the fact that at  $1000^\circ C$ , e.g., the single phase  $M_3O_8$  is obtained with virtually the same O/M ratio for  $y = 0$  and  $y = 0.05$ . Furthermore, two phase samples with a noticeable proportion of cubic phase are found at all temperatures at or near oxygen contents inside the  $M_3O_8$  single phase region as proposed by MARKIN and STREET.

It is to be noted further that we determined a rather different position of the tie-lines in the  $M'_{3}O_{8-z} + M''O_{2+x}$  two phase region than that given by MARKIN and STREET, on the basis of their own and of BRETT and FOX' (4) results. In particular, no tie-line was observed by us extending to very high plutonium contents as in the work of BRETT and FOX. Tie-lines parallel to lines of constant  $y$ , as given by MARKIN and STREET for room temperature, were not found by us except for the metastable  $600^{\circ}\text{C}$  phase diagram.

References

- (1) T.L. MARKIN, R.S. STREET, J.Inorg.Nucl.Chem. 29, 2265-80 (1967).
- (2) The Plutonium-Oxygen and Uranium-Plutonium-Oxygen Systems: A Thermochemical Assessments, IAEA Tech.Rep.Series No. 79, Vienna 1967, p. 54-9.
- (3) G. DEAN, Plutonium 1965, Chapman and Hall, London 1965, p. 806-27.
- (4) N.H. BRETT, A.C. FOX, J.Inorg.Nucl.Chem. 28, 1191-1203 (1966); AERE-R 3937 (1963).
- (5) C. SARI, U. BENEDICT, H. BLANK, Thermodynamics of Nuclear Materials 1967, IAEA Vienna 1968, p. 587-611.
- (6) T.L. MARKIN, E.J. McIVER, Plutonium 1965, Chapman and Hall, London 1965, p. 845.
- (7) U. BENEDICT, EUR 3897 d (1968).
- (8) P. PERIO, Bull.Soc.Chim.France 20, p. 840-1 (1953).
- (9) Thermodynamics and Transport Properties of Uranium Dioxide and related Phases, IAEA Tech.Rep.Series No. 39, Vienna 1965, p. 19-21.
- (10) B. CHODURA, J. MALY, Proc. 2nd Geneva Internat. Conf. 1958, P/2099.
- (11) A.F. ANDRESEN, Acta Cryst. 11, p. 612-14 (1958).
- (12) B.O. LOOPSTRA, Acta Cryst. 17, p. 651 (1964).
- (13) S. SIEGEL, Acta Cryst. 8, p. 617-19 (1955); Powder Diffraction File 8-244.
- (14) H.R. HOEKSTRA, S. SIEGEL, L.H. FUCHS, J.J. KATZ, J.Phys.Chem. 59, p. 136-8 (1955).
- (15) S. STEEB, Z. Metallkunde 55, p. 445-52 (1964).



Legend for the phase diagrams figs. 1, 6, 8 and 11 :

---

- orthorhombic  $M_3O_{8-z}$
- orthorhombic  $M_3O_{8-z}$  + f.c.c.
- single phase f.c.c.
- × two f.c.c. phases
- tetragonal (" $M_3O_7$ ") phase
- ▣ orthorhombic  $M_3O_{8-z}$  + tetragonal phase
- △ f.c.c.  $MO_{2.0}$  + tetragonal phase

- )
- .-.-.-.-, ) phase limits
- )
- tie-lines
- ..... oxidation limit in air

Figures 2 or 3 on an experimental point means overlapping of 2 or 3 measurements.

The phase relations for  $O/M < 2.00$  were omitted from the diagrams.

ACKNOWLEDGEMENTS

The authors would like to thank Dr. H. Blank for helpful and stimulating discussions. They are indebted to the Ceramics Section and to the Analytical Chemistry Section for preparation and chemical analysis of the starting material.

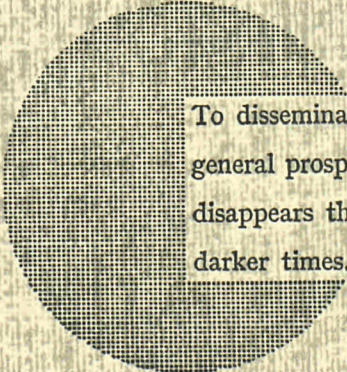
#### NOTICE TO THE READER

All Euratom reports are announced, as and when they are issued, in the monthly periodical "euro-abstracts", edited by the Centre for Information and Documentation (CID). For subscription (1 year : US\$ 16.40, £ 6.17) or free specimen copies please write to :

**Handelsblatt GmbH**  
"euro-abstracts"  
Postfach 1102  
D-4 Düsseldorf (Germany)

or

Office de vente des publications officielles  
des Communautés européennes  
37, rue Glesener  
Luxembourg



To disseminate knowledge is to disseminate prosperity — I mean general prosperity and not individual riches — and with prosperity disappears the greater part of the evil which is our heritage from darker times.

Alfred Nobel

## SALES OFFICES

All reports published by the Commission of the European Communities are on sale at the offices listed below, at the prices given on the back of the front cover. When ordering, specify clearly the EUR number and the title of the report which are shown on the front cover.

### SALES OFFICE FOR OFFICIAL PUBLICATIONS OF THE EUROPEAN COMMUNITIES

37, rue Glesener, Luxembourg (Compte chèque postal N° 191-90)

#### BELGIQUE — BELGIË

MONITEUR BELGE  
40-42, rue de Louvain - 1000 Bruxelles  
BELGISCH STAATSBLAD  
Leuvenseweg 40-42 - 1000 Brussel

#### LUXEMBOURG

OFFICE DE VENTE  
DES PUBLICATIONS OFFICIELLES  
DES COMMUNAUTES EUROPEENNES  
37, rue Glesener - Luxembourg

#### DEUTSCHLAND

BUNDESANZEIGER  
Postfach - 5000 Köln 1

#### NEDERLAND

STAATSDRUKKERIJ  
Christoffel Plantijnstraat - Den Haag

#### FRANCE

SERVICE DE VENTE EN FRANCE  
DES PUBLICATIONS DES  
COMMUNAUTES EUROPEENNES  
26, rue Desaix - 75 Paris 15<sup>e</sup>

#### ITALIA

LIBRERIA DELLO STATO  
Piazza G. Verdi, 10 - 00198 Roma

#### UNITED KINGDOM

H. M. STATIONERY OFFICE  
P.O. Box 569 - London S.E.1

Commission of the  
European Communities  
D.G. XIII - C.I.D.  
29, rue Aldringer  
Luxembourg

CDNA04136ENC